Atmos. Chem. Phys. Discuss., 10, 5665–5716, 2010
www.atmos-chem-phys-discuss.net/10/5665/2010/

Atmospheric Chemistry and Physics Discussions

This discussion paper is/has been under review for the journal Atmospheric Chemistry and Physics (ACP). Please refer to the corresponding final paper in ACP if available.

Variability and budget of CO_2 in Europe: analysis of the CAATER airborne campaigns – Part 1: Observed variability

I. Xueref-Remy[1], C. Messager[1], D. Filippi[2], P. Nedelec[3], M. Ramonet[1], J. D. Paris[1], and P. Ciais[1]

[1]Laboratoire des Sciences du Climat et de l'Environnement/Institut Pierre Simon Laplace, UMR1572, CEA Orme des Merisiers, 91191 Gif-sur-Yvette CEDEX, France
[2]Sextant Technology Ltd, 116 Wilton Road, Wellington 6012, New Zealand
[3]Laboratoire d'Aérologie, 14 avenue Edouard Belin, 31400 Toulouse, France

Received: 23 September 2009 – Accepted: 29 December 2009
– Published: 26 February 2010

Correspondence to: I. Xueref-Remy (irene.xueref@lsce.ipsl.fr)

Published by Copernicus Publications on behalf of the European Geosciences Union.

Abstract

Atmospheric airborne measurements of CO_2 are very well-suited to estimate the time varying distribution of carbon sources and sinks at the regional scale. We present here an analysis of two cross-European airborne campaigns that have been carried out on 23–26 May 2001 (CAATER 1) and 2–3 October 2002 (CAATER 2) over Western Europe. The area covered during CAATER 1 (respectively CAATER 2) was comprised between longitude 4° W to 14° E and latitude 44° N to 52° N (respectively longitude 1° E to 17° E and latitude 46° N to 52° N). High precision in-situ CO_2, CO and Radon 222 measurements have been recorded. Flasks samples have been collected during both campaigns to cross-validate the in-situ data. During CAATER 1 (respectively CAATER 2), the mean CO_2 concentration was 370.1±4 ppm (respectively 371.7±5 ppm). A HYSPLIT backtrajectories analysis shows that during CAATER 1, dominant winds were blowing from the north-west. In the planetary boundary layer (PBL) airmasses got contaminated over Benelux and Western Germany by pollution from these high urbanized areas, reaching about 380 ppm. Air masses passing over rural areas are depleted in CO_2 because of the photosynthesis activity of the land cover vegetation, as low as 355 ppm. During CAATER 2, the backtrajectory analysis shows that airmasses were distributed among the 4 sectors. Airmasses got enriched in CO_2 and CO when passing above polluted spots in Germany but also in Poland, as these countries are known to hold part of the most polluting plants based on coal consumption, the so-called "dirty thirty" from WWF. Simultaneous measurements of in-situ CO_2 and CO combined to backtrajectories helped us to discriminate the role of fossil fuel emissions from over CO_2 sources. The $\Delta CO/\Delta CO_2$ ratios (R^2=0.33 to 0.88, slopes=2.42 to 10.37), calculated for polluted airmasses originating from different countries/regions, matched quite well national inventories, showing that the airborne measurements can help to identify the role of fossil fuel sources even several days/hundreds of kms further in the PBL. CO_2 observations have been compared to surrounding ground stations measurements, confirming that the stations located near the ground (ex. CBW, WES, HUN)

ACPD

10, 5665–5716, 2010

are representative of the local scale, while those located in the free troposphere (FT) are representative of atmospheric CO_2 on a regional scale of a few hundred kilometers (ex. CMN). Stations located several 100 km away measure CO_2 concentrations different from a few ppm, indicating the existence of a gradient of a few ppm in the free troposphere. Observations at stations located on top of small mountains (ex. SCH, PUY) match or not the airborne data whether they sample air from the FT or air coming up from the valley. Finally, the analysis of the CO_2 vertical variability conducted on the 14 profiles recorded per campaign shows that is at least 5 to 8 times higher in the PBL (4 ppm and 5.7 ppm for CAATER 1 and CAATER 2, respectively) than in the FT (0.5 ppm and 1.1 ppm for CAATER 1 and CAATER 2, respectively). The CO_2 jump between the PBL and the FT equals 3.7 ppm for the first campaign and −0.3 ppm for the second campaign. A very striking zonal CO_2 gradient of about 11 ppm could be observed in the mid-troposphere during CAATER 2, with higher concentrations in the West than in the East. This gradient could originate from differences in atmospheric mixing, ground emission rates or a earlier beginning of the Fall in the west. More airborne campaigns are currently under analysis in the framework of the CARBOEUROPE-IP project to better assess the role of these different hypothesis. In a companion paper (Xueref-Remy et al., 2010), a comparison of vertical profiles from observations and several modeling frameworks is conducted for both campaigns. An attempt to calculate CO_2 fluxes during CAATER 1 using CO_2 and Radon-222 observations and modeling tools is also carried out.

1 Introduction

Atmospheric greenhouse gas concentrations have been increasing since the pre-industrial era, due to human activities such as the combustion of fossil fuel compounds and deforestation. CO_2 is the main additional gas, its atmospheric concentration having increased of more than 30% during the last 150 years. Political decisions have been made in the aim of reaching a stabilization of atmospheric CO_2 concentration through

ACPD
10, 5665–5716, 2010

the United Nations Framework Convention on Climate Change. Such decisions require an independent verification of anthropogenic and natural fluxes of each country, which represent a huge scientific and political challenge (IPCC, 2007).

The atmosphere is a strong integrator of CO_2 surface sources and sinks. Observations can thus be used to quantify surface fluxes over more or less large scales by matching them with modelled fields simulations from transport models. This method, known as inverse modelling, is the approach the most used to quantify CO_2 fluxes at regional or global scales. However, the flux partition, especially at the regional scale (100–1000 km) is still poorly known. Indeed for Europe (based on data from 1992–1996), Gurney et al. (2003) have compared 16 inverse models: all indicate that Europe is a sink for CO_2 but they show very large differences, with a mean annual flux of 0.6 Gt C/yr and a standard deviation of ±0.4 Gt C/yr i.e. 66% of the mean.

Briefly, these large differences originate from several reasons, among which a lack of measurements over the continents to constrain fluxes calculations by inverse modelling (Geels et al., 2007). Also, models have difficulties to represent atmospheric transport in the continental planetary boundary layer (PBL) (Gerbig et al., 2003). Several intercomparison studies have been made to make progresses in the modeling of the fluxes and especially on the seasonal scale (e.g. Gurney et al., 2004; Baker et al., 2006; Law et al., 2008; Patra et al., 2008; Carouge et al., 2008a, b).

Globally at this stage, reducing inverse modelling uncertainties requiere to better characterize atmospheric CO_2 vertical and horizontal variability through in-situ observations. Over the 10 past years, the global monitoring network of atmospheric CO_2 has been largely used to retrieve the large scale distribution of sources and sinks at the surface. The most recent studies have demonstrated the need for more data over the continental region, to make feasible robust estimations of the biospheric contribution to the regional carbon budget. In a recent paper, Stephens et al. (2007) have especially put in light the need for in-situ vertical observations to better constrain CO_2 fluxes. Indeed, because of the large space they can span within a reduce time, airborne measurements are very well suited to study the atmospheric CO_2 variability at

ACPD
10, 5665–5716, 2010

the regional scale, vertically and horizontally, and can especially give crucial information on the gradients between the PBL and the FT. Over Europe, airborne campaigns conducted in the boundary layer are very poor as resumed in Geels et al. (2007). The Co-ordinated Access to Aircraft for Transnational Environmental Research (CAATER 1 and CAATER 2), an European initiative, has given us the opportunity to perform two intensive airborne campaigns over Western Europe in May 2001 and October 2002.

The aim of these campaigns were: 1) to validate a new airborne in-situ CO_2 analyzer; 2) to characterize the CO_2 variability in the low troposphere above Western Europe; 3) to evaluate the respective contributions of anthropogenic and biospheric fluxes to this variability; 4) to assess the representativness of ground stations; and 5) to better characterize the gradients of CO_2 between the boundary layer (PBL) and the free troposphere (FT).

In this paper, we show the results of these campaigns that occured in the low troposphere (<4000 m) aboard the Falcon 20 of the Deutsches Zentrum für Luft und Raumfahrt (Oberpfaffenhofen Germany). During this experiment the Falcon was equipped with a continuous CO_2 analyser (CONDOR), a continuous CO analyser (MOZAIC CO analyser, Laboratoire d'Aérologie, France) which was used as a combustions tracer and a sequential Radon 222 analyser (AVIRAD) which was used as a tracer of continental airmasses.

The campaigns conditions and the instrumentation are presented in Sect. 2. In Sect. 3, we conduct an analysis of air mass origins using backtrajectories. In Sect. 4, we analyse the contribution of polluted air masses in CO_2 variability using CO data. In Sect. 5, we assess the representativness of ground stations measurements using aircraft observations. Finally Sect. 6 focuses on CO_2 vertical variability, especially on characterizing CO_2 gradients between the PBL and the FT in function of the airmass origins. In a companion paper (Xueref-Remy et al., 2010), we conduct a comparison between observations and models: first to assess the performances of a global model versus a mesoscale model to reproduce the observed gradients, testing also several biospheric fluxes. And second, to present a comparison between model-based fluxes

ACPD
10, 5665–5716, 2010

obtained from a new method coupling backplumes and a priori fluxes, and observation-based fluxes calculated with the Radon method (Schmidt et al., 2003).

2 Description of the campaigns and of the instrumentation

2.1 The CAATER campaigns

The CAATER aicraft measurement (Co-ordinated Access to Aircraft for Transnational Environmental Research) programme is coordinated by the German DLR, French INSU/CNRS and Météo-France, and by the UK Met Office. This programme has been funded between 2000 and 2003 by the European Commission to provide access to research aircraft facilities to research laboratories for pilot projects and new studies. The objectives of the CAATER Carbon Dioxide pilot project detailled in this study is to measure the vertical and horizontal variability of CO_2 over Western Europe during two contrasted seasons. We used the DLR-Falcon 20 jet aircraft (http://www.dlr.de/fb/en/desktopdefault.aspx/tabid-3714/5789_read-8405/) equipped with 1) a CO continuous infra-red analyzer, 2) a CO_2 non dispersive infra-red gas analyzer, 3) a 222Rn sequential sampler instrument, 4) a flask sampling unit and 5) standard meteorogical parameter sensors.

Two airborne campaigns were carried out in May 2001 and in October 2002, here called CAATER-1 and CAATER-2, respectively. The two flight routes are different, but they both extend roughly across a domain of roughly 20° in longitude between Western France and West Hungary. The Falcon-20 flights of each campaign are shown in Fig. 1. The CAATER-1 campaign consists of 5 flights for a total of 14 h during 23–26 May 2001, and the CAATER-2 campaign consists of 3 flights for a total of 8 hrs during 2–3 October 2002 (Tables 1 and 2). Vertical CO_2 profiles (and in CAATER-2 additionally of CO and 222-Rn) were collected between the ground and 4000 m during each campaign. We have in total 14 profiles for each campaign.

ACPD
10, 5665–5716, 2010

Because the focus of this study is to analyze the variability of CO_2 across Western Europe, it is important to have information of the underlying fluxes, which we provide in this section. Figure 1 shows the average CO_2 flux maps over Western Europe during the sampling interval of each campaign. The net CO_2 flux is the sum of fossil fuel CO_2 emissions and of the Net Ecosystem Exchange flux, which can be positive (source) or negative (sink) depending upon the vegetation status. The Normalized Difference Vegetation Index (NDVI) provided by the SPOT VGT-4 satellite system reveals a higher photosynthetic activity during May than during October (see Appendix A), but vegetation index is not easy to translate into a CO_2 source/sink map. We show in Fig. 1, overlaid with the campaign flights, the Net Ecosystem Exchange (NEE) fluxes given by the process-based ecosystem model ORCHIDEE (Krinner et al., 2005) with a spatial resolution of $0.35^\circ \times 0.35^\circ$; also described in the companion paper (Xueref-Remy et al., 2010) forced by synoptic weather data with a 3 h resolution, averaged on the days of the campaign (the diurnal cycle thus being smoothed), as well as annual fossil fuel (FF) emission maps with a spatial resolution of $1^\circ \times 1^\circ$ from Andres et al. (1996) updated to the year of each campaign and oceanic fluxes from Takahashi (1999, 2002). As oceanic fluxes are negligible compared to NEE and fossil fuel fluxes, they do not appear in the maps. These maps show that in this period of May 2001, Europe was mainly acting as a CO_2 sink (reaching about -1 g C m^{-2} day^{-1}) while early October 2002 it was acting more like a source of CO_2 northern of 47° N (about 1 g C m^{-2} day^{-1}) and a tiny sink southern of 45° N (about 0.4 g C m^{-2} day^{-1}). Largest fossil fuel emissions occur from London megacity, Benelux, Ruhr, Berlin megacity and Varsow city regions. They are identified to hold part of the most polluting power plants based on coal consumption (the so-called "dirty thirty" from WWF: http://www.panda.org/what_we_do/knowledge_centres/climate_change/problems/cause/coal/dirty_30/, that represent 10% of european CO_2 emissions].

The paper is also using a dataset from different in-situ sampling sites that are described in Table 3.

ACPD
10, 5665–5716, 2010

2.2 Synoptic weather conditions

Synoptic weather conditions encountered during both campaigns are shown in Fig. 2 (http://weather.ou.edu/~cgodfrey/reanalysis/).

During CAATER 1, the synoptic situation was mainly anti-cyclonic, as shown by mean sea level pressure and 850 hPa wind maps. Note that 850 hPa defines the mean aircraft altitude during the campaign. No major cloud system was present over Europe during the campaign. During 23–24 May 2001 a flow from the North East prevailed over the campaign domain in Northern France, established around a high-pressure system located over the British Isles. During 25 May, as this high-pressure moved towards southern Scandinavia, north-easterly winds prevailed.

During CAATER 2, dry conditions were encountered, appart for 3 October 2002 when a few showers occured over Thüringen, in Eastern Germany. By 2 October 2002, a small high-pressure system over Norway induced a flow from the North into the aircraft route over Southern Germany. But another high-pressure placed over the Balkans region creates a second flow from Southern Europe into the aircraft route over France. We thus expect a drastic change in air mass origins at the boundary between these two different flow regimes. On 3 October 2002 two high-pressure systems can be observed, respectively West and East of the aircraft route, one over France and another over Greece. This situation gives rise to complex wind patterns, as further evidenced from the backtrajectory analysis in Sect. 3.

2.3 Instrumentation

2.3.1 In situ continuous CO_2

In addition to standard meteorological parameters (wind, relative humidity, temperature, pressure) with a 1-Hz acquisition, the CO_2 concentrations were measured with a continuous NDIR airborne analyzer developed at LSCE (Fig. 3). This instrument is based on a commercial sensor Li-COR 6262 with a fast response detector (1 Hz

acquisition), with temperature, pressure and flow rates of air being regulated at constant values (Table 4). Outside air is pumped and dried by a magnesium perchlorate cartridge before being analyzed. More details can be found in Filippi (2002).

Airborne CO_2 measurements are useful for carbon cycle studies (inversions) if they have a precision better than 0.5 ppm (Gloor et al., 2000). Frequent calibrations (each 30 min) allow to reach an instantaneous precision of 0.1 ppm, but slow instrument drifts due to changes in surrounding physical parameters such as pressure and temperature require frequent calibrations during flights. We used two calibration gases in high-pressure cylinders of 2 L, with concentrations in the NOAA X-93 scale of 365.92±0.045 ppm (Low) and 401.29±005 ppm (High). Each standard is passed during 3 min in the analyzer, and only the last minute of acquisition is kept to calculate outside air CO_2. Given the limited volume of each cylinder, the time taken for calibration and the sought precision, an optimal compromise had to be found. We carried out ≈30 calibrations during each campaign. The average stability (1-σ std. deviation on 1-Hz data) was 0.03 ppm during the last minute of each calibration passage. To compute the instrument accuracy, each calibration gas was treated as an unknown target. The difference between the true and the measured target value is 0.1 ppm for the high standard and 0.08 ppm for the low one. Also, we tested that, even when using one single calibration result before each flight, the instrument accuracy is still greater than 0.2 ppm.

Figure 4 provides CO_2 as a function of altitude, longitude and latitude to give a 3-D view of the CO_2 concentration measured during both campaigns. The content of this figure is analyzed in the following at two places: first in Sect. 3, we make an analysis of the CO_2 horizontal distribution through a projection of Fig. 4 on the latitude-longitude plane. Then in Sect. 6, an analysis of the CO_2 vertical distribution through a projection of Fig. 4 on the altitude-longitude plane is developed.

ACPD
10, 5665–5716, 2010

2.3.2 Flasks

To independently assess the instruments accuracy, about 50 1-L glass flasks have been sampled during each campaign. After 5 min of flushing, the sampled air is compressed at 1 bar above atmospheric pressure to avoid any contamination due to leakage. The CO_2 concentration was determined at the LSCE by gas chromatography with a precision <0.1 ppm (Pépin et al., 2001), each flask being measured twice. A flask concentration was systematically rejected if both measurements were different by more than 0.1 ppm (3.2% of the samples). The mean difference between the in-situ NDIR and the flasks is less than 0.2 ppm for both campaigns (see Appendix B, Fig. B1).

2.3.3 In situ continuous CO

The CO instrument is the same analyser than the one developed for routine measurements onboard passenger aircrafts for the MOZAIC program (http://mozaic.aero.obs-mip.fr/web/). CO was only measured during CAATER-2 and its characteristics are summarized in Table 4. The analyser (Nedelec et al., 2003) is a fully automated instrument designed to reach an accuracy of 5%. It is based on the commercial IR correlation gas analyser Model48C produced by Thermo Environment Instruments (TEI, USA). It is a Gas Filter Correlation instrument on the principle of infra-red absorption by the 4.67 µm fundamental vibration-rotation band of CO. Radiation from an infrared source is chopped and passes through a gas filter which alternates between CO and N_2 due to rotation of the filter wheel. The radiation then passes through a narrow band pass filter and a multiple optical pass sample cell where absorption by the sample gas occurs. The IR radiation exits the sample cell and falls on a PbSe solid state IR detector. Other gases do not cause modulation of the detector signal since they absorb the reference and measure beams equally. Thus, the Gas Filter Correlation System responds specifically to CO. The Model 48CTL is also qualified by US EPA designated Method (EQSA-0486-060). The specification of the commercial instrument is 10 ppbv CO for 300 s integration time. Major improvements have been brought by Nédélec et

ACPD
10, 5665–5716, 2010

al. (2003): periodic accurate zero measurements, new IR detector with better cooling and temperature regulation, pressure increase and regulation in the absorption cell, increased flow rate to 4 l/min, water vapour trap, and ozone filter. The specifications achieved for 30 s integration time (response time of the instrument) are a precision of ±5 ppbv CO with a minimum detectable of 10 ppbv of CO. The instrument has been calibrated before and after the campaign with a traceable CO cylinder from the National Institute of Standards and Technology in Boulder, Colorado, USA.

2.3.4 Semi-continuous Radon-222 daughters sampler

Radon has been measured with the AVIRAD instrument (Filippi, 2000), which consists of an isokinetic probe fixed on the fuselage and of a filtration unit located inside, with limited and straight tubing between the probe and the filter. The isokinetic probe was built by Sextant Avionique Corporation on the same design used for the NASA C-141 (Kritz et al., 1998). The radon measurements are made with alpha spectrometry of the radon progeny products deposited on the collected aerosols. The Paper Filtering Unit is provided with 4 Si detectors in order to measure the alpha activity of each sample at 4 successive decay times. The Data Acquisition System runs 4 alpha spectrometers allowing implementation of different methodologies to validate the radon concentration data. The probe includes a stagnation reservoir, the null-type air inlet and a flow line sensor. It was mounted on the cargo window, under the airplane. At the location of the probe, the boundary layer of the plane was expected to be less than 10 cm. Thus in order to keep the air inlet beyond the boundary layer of the plane, it was fixed at the tip of a 29-cm long mast. The null-type nozzle operates by measuring static pressure on the outside of the probe nozzle, and static pressure inside the inlet opening of the nozzle. When zero pressure differential is developed between the inside and outside pressure taps, the isokinetic velocity is obtained. This null differential pressure is automatically adjusted in real-time. The null-type nozzle was calibrated in wind tunnel for the Mach number range of the aircraft, between Mach number 0.6 and 0.7. At the rear part of the air inlet, a flow line sensor made of 4 dynamic pressure taps is used during test flights

ACPD
10, 5665–5716, 2010

to make sure that the angle of attack of the isokinetic nozzle was as close as possible to zero. The flow line sensor was also calibrated in wind tunnel for the Mach number range of the aircraft. Except during turns and turbulences, the angle of attack of the probe was less than 2 degrees, even during ascents and descents. The Filter Unit used a continuous paper filter strip which is advanced by a motorysed take-up spool at programmable time intervals. To preserve the collected samples, a blank strip is rolled up along with the filtering strip on the take-up spool. Different paper filter media can be used depending on subsequent analytical procedure. The number of samples per spool is about 70. The active area of each sample is 1700 mm^2. The precision of the measurement is 30%.

3 Origin of sampled air masses

3.1 Mean CO_2, CO concentrations and backtrajectories

The CO_2 distribution observed over the European continent results from the mixing of oceanic background air with continental signals from fossil fuel emissions and biospheric sources and sinks. The lower tropospheric CO_2 mean concentration between 0–4000 m is 370.1±4 ppm during CAATER-1 (May) compared to 371.7±5 ppm during CAATER 2 (October). Thus, despite a stronger biogenic uptake in Spring, reducing both background CO_2 over the whole Northern Hemisphere and CO_2 over the European continent, the lower troposphere mean level in May is roughly similar to October. For CAATER-2, the mean CO concentration was 177±61 ppb.

As a reference for our analysis, we give the marine background value of CO_2 and CO (averaged over each campaign duration), determined from the record of the Mace-Head station located on the West coast of Ireland (marine sector clean-air selection) (GLOBALVIEW-CO2, 2006, and GLOBALVIEW-CO, 2006): CO_2 marine background concentration were 374.5±0.3 ppm during CAATER 1 and 367.9±0.2 ppm during CAATER 2, and CO marine background was 131.1±0.2 ppb during CAATER 2.

ACPD
10, 5665–5716, 2010

In order to better investigate the origin of the sampled air masses, we computed for each flight a set of 5-days backtrajectories using the Hysplit-4 model (Draxler and Hess, 1998). The wind fields are the 6-hourly archive data from the NCEP operational model analysis (FNL archive data) with an horizontal resolution of 1° × 1° and 14 vertical levels.

3.2 Air masses sampled in May 2001 during CAATER-1

Backtrajectories calculated for each flight of CAATER 1 are shown in Fig. 5 (a projection of Fig. 4 for CAATER 1 in the horizontal latitude-longitude plan). About 58% of the air masses sampled came from the north-west, 37% from the north-east (37%) and only 5% from the south-east.

On 23 May 2001 (Fig. 5a), between 2° W and 4° E, the back-trajectories indicate a continental origin from the north-east, with air masses being advected in the boundary layer (<2000 m) and carrying low CO_2 values of ≈360 ppm. These low values likely reflect recent plant uptake. As the aircraft moved west of 2° W, the sampled air mass became exposed to fossil fuel emissions over urbanized parts of Netherlands and southern Germany (Ruhr), and thus got suddenly enriched in CO_2 (reaching about 380 ppm). Roughly speaking, the signal of this high emission region of Europe as compared to the "biospheric" minimum further east is hence on the order of 20 ppm in the whole boundary layer.

On 24 May (Fig. 5b) over the Sea of Biscay, air masses were locally polluted near the surface close to BZH (~378 ppm). The aircraft flight over the sea of Biscay first sampled air advected from the Channel sea at ≈4000 m with oceanic CO_2 concentrations of 372–374 ppm, and then more continental air from north eastern Europe, with CO_2 depleted by plant uptake down to 360 ppm.

On 25 May (Fig. 5c), the air mass was first oceanic (374 ppm). Moving eastwards between 3° W and 1° E, continental air masses were sampled with $CO_2 \approx 360$ ppm, then oceanic air, followed again by polluted air over the Ruhr region with $CO_2 \sim 380$ ppm. The polluted and biospheric CO_2 values are extremely similar to those sampled during

ACPD
10, 5665–5716, 2010

May 23 on roughly the same route westwards.

On 26 May (Fig. 5d), we measured at 12° E the lowest CO_2 concentrations (355 ppm) of the whole campaign into an air masses that clearly came from the East. In contrast, air masses coming from the west and north-west, which were exposed to more urban areas are associated with CO_2 higher by 25 ppm above this minimum. Note that the easterly flow which was associated with minimum CO_2 values corresponds to air masses advected into the boundary layer, and thus directly exposed to continuous biospheric uptake.

3.3 Air masses sampled in October 2002 during CAATER-2

The CAATER 2 back-trajectories are shown in Fig. 6 (a projection of Fig. 4 for CAATER 2 in the horizontal latitude-longitude plan): 33% of the sampled airmasses are from the south west, 26% from the south east, 22% from the north west and 19% from the north east. The source regions influencing the CAATER-2 campaign are thus more diverse than for CAATER 1. Figure 7 shows CO and CO_2 aircraft observations as a function of time (~800 km between OBP and PDB via ORL for 2 October, and ~1500 km between THU and OBP via HUN). Due to anthropogenic combustions, the observed European lower troposphere CO concentration equals 160 ppb (from the surface to ~1200 m), being 30 ppb higher than the MHD marine background.

On 2 October, in the flight from OBP to ORL (Fig. 6a), a pollution plume is sampled after take-off (event C1 in Fig. 7) with a significant positive CO_2 vs. CO correlation (Table 5). Between 10 and 8° E the sampled air mass origin is from the north east, associated with highly variable CO_2 and CO (Fig. 7). During the B1 ascent over South West Germany (Fig. 7; above SCH mountain station) the aircraft flying altitude increases from 1000 m to 1800 m. In parallel, CO is dropping from 130 ppb down to 110 ppb and CO_2 is increasing from 363 ppm up to its background value (370 ppb). The corresponding CO levels match with observations made the same day above München (germany) within the MOZAIC program, where concentrations of CO dropped down from about 200–300 ppb below 1 km to about 100–110 ppb around 1.5 km of altitude

(P. Nedelec, personal communcation). Crossing the polluted air mass C2 near 5.5° E, a high correlation between CO_2 and CO is observed (Fig. 7). Hysplit-4 backtrajectories show that airmasses sampled in C2 were originating from the north east, then over Germany they looped before reaching the aircraft position by passing over the Rhone valley at a low altitude level (about 500 m a.s.l.). The air mass sampled in C2 is thus likely impacted by anthropogenic CO and CO_2 emissions from the Rhone valley. West of 5.5° E, back-trajectories indicate air masses from Southern France.

On 2 October, during the flight from ORL to PDB (Fig. 6b; Table 2) a vertical profile is sampled over ORL (event B2 in Fig. 7). In this B2 profile, CO_2 is vertically homogeneous at ≈374 ppm but CO decreases above 1 km from 180 ppb to 70 ppb at 4000 m, i.e. to a value much lower than the marine background value. Backtrajectories show that this air originated from higher levels. Indeed, on 2 and 3 October, profiles recorded in the region of München in Germany between the ground level and about 12 km of altitude in the framework of the MOZAIC project show a dramatic decrease of CO from 200 to 300 ppb below ∼1 km of altitude to less than 80 ppb above that level (P. Nedelec, personal communication). Thus we likely sampled air from the background mid to high troposphere. East of ORL (event M3 in Fig. 6), elevated and variable CO_2 and CO concentrations are observed with a south-western, and then a southern, low altitude origin. The air mass sampled in M3 is likely influenced by pollution sources from the Rhone valley and from urban regions of the French mediterranean coast. There is no strong correlation, however, between CO and CO_2 in the M3 event (R^2=−0.42). During the aircraft route over South-Germany (event B3 in Fig. 7) the aircraft climbed up and we observe again background values of CO_2 and CO. During the last part of the 2 October flight, East of 6.5° E and mostly in the boundary layer (event M4 in Fig. 7) CO varies from 140 to 305 ppb and CO_2 from 358 to 385 ppm. This huge horizontal variability is associated with an air-mass descent from the North-East passing over a cities and rural regions in Denmark and Eastern Germany (see Fig. 6).

On 3 October, during the flight from OBP to HUN (Table 2; Fig. 6c) a vertical profile is sampled over a rural location in the Thüringen area (event B4 in Fig. 7). This profile

shows CO_2 and CO values close to background. The same tropospheric values at 4000 m than those measured one day earlier over ORL shows that the signal of sources and sinks is mainly confined into the boundary layer during the CAATER-2 campaign, because of anticyclonic conditions and reduced mixing. A pollution event (event C3 in Fig. 7) is recorded between 12° and 13.5° E, with some positive CO-CO_2 correlation (R^2=0.26, slope=1.78). In this C3 event, the air masses origin can be traced to the high emission Ruhr industrial region. Over HUN at 17° E (event C4 in Fig. 7) we encountered another well-defined pollution plume (R^2=0.47, slope=3.2) during the vertical profile over the tall tower of Hegyatsall.

On 3 October, during the (return) flight from HUN to OBP (Fig. 6d), the aircraft climbed above 4000 m (event B6); background values of CO, CO_2 at 4000 m are checked to be unchanged from the flight above Orleans' forest (event B2). Then, an horizontal route is followed in the boundary layer (mean altitude 300 m; event C5 in Fig. 7). Near-surface pollution sampled West of HUN (R^2CO-CO_2=0.88, slope=10.37) is most likely of local origin, from the Graz city (it is the second city of Austria with 300 000 people and an international airport). Finally, the airplane crossed Eastern Germany westwards to OBP at 2200 m altitude. Surprinsingly low CO_2 values being recorded for the month of October (360 ppm) are observed during that last flight, as well as low CO values (110 ppb). The backtrajectories of this flight show a complex pattern, with air partly coming from the Alps before reaching the aircraft position.

4 Relationship between CO and CO_2 in polluted air masses

We now analyze the relationship between CO and CO_2 observed during the CAATER 2 campaign (unfortunately, no CO data available for CAATER 1). We expect a positive correlation between CO and CO_2 in air masses influenced by combustion processes, which in turn should open the possibility to separate fossil fuel CO_2 from total CO_2 in sampled air masses (e.g. Levin and Karstens, 2007). This (too) simple theory is however complicated by 1) different CO:fossil CO_2 emission ratios determined by the

ACPD
10, 5665–5716, 2010

efficiency of various types of combustion, 2) mixing of fossil fuel CO_2 rich air with oceanic or vegetation fluxes, a process that changes CO_2 without changing CO, and 3) chemical production of secondary CO from biogenic organic volatile compounds, which in summer can contribute as much CO as anthropogenic combustions (Rivier et al., 2006); this process acts to increase CO and not change CO_2. In pollution loaded air masses sampled downwind of China or the US, a strong positive relationship between CO and CO_2 has been characterized by aircraft campaigns (Crawford et al., 2003; Suntharalingam et al., 2004; Paris et al., 2008). In some cases, the observed linear regression slope between CO and CO_2 can even be used to constrain the flux of one tracer, knowing the one of the other (Palmer et al., 2006). Here in Western Europe for the CAATER-2 campaign domain, the three above "complicating" processes (different mix of combustion, mix of oceanic, vegetation and fossil fuel CO_2, secondary CO production) are unfortunately at work. This in principle conceals the separate inference of fossil CO_2 very difficult, as already noted when using ground-based stations records (Karstens et al., 2006; Levin et al., 2007). In this context, it is interesting to check in the CAATER-2 campaigns which sampled diverse air masses (see Sect. 3), the relationship between CO and CO_2.

First, we identify in the CAATER-2 dataset the different air masses classified from their distinct origins in Fig. 6. Then we compute for each air mass the linear regression correlation (R^2 determination factor) and slope (S) of ΔCO_2 vs. ΔCO (delta stands for the difference to background concentration). The results are presented in Fig. 8. The R^2 and slope values show a wide range of variation when all air masses are considered without distinction (Table 5). We then select only the well-identified polluted air masses diagnosed from back-trajectories (events C1 to C5). These polluted air masses all show high R^2 values (0.33 to 0.88), but their slope varies from 2.42 to 10.37 (Table 5). These slope values are compared below to the CO:CO_2 slope ρ given by emission inventories (EMEP, 2008) in the region of influence of each air mass.

Air mass C1 is exposed to fossil fuel emission fluxes in Eastern Germany/Western Poland/Southern Sweden (see Sect. 3). It has the highest R^2, and a slope S=6.38

higher than the mean inventory derived slope in Germany (ρ=5.1). One can see in Fig. 6a that C1 is not only influenced by Eastern Germany, but also by industrial regions (Malmö) in Southern Sweden and in Western Poland, where the CO:CO_2 emission ratio are regionaly higher (range 11.1 to 12).

Air mass C2 is exposed to Rhone valley emissions as well as to vegetation CO_2 uptake in that region (Sect. 3; see also the high NDVI values in Fig. A1). This air mass shows a weak CO_2-CO correlation (R^2=0.65) and a lower slope (3.52) than expected from fossil fuel addition alone (France CO:CO_2 emission inventory ratio ρ=14), indicating a strong biospheric contribution reducing CO_2 while leaving CO unaffected.

Air mass C3, sampled at ~900 m, is exposed to South Germany emissions (Fig. 6c). The R^2 factor is not very high (0.26) and the slope is 1.78, quite low compared to 5.1 for the emission inventory ratio for Germany, meaning that these emissions have been likely diluted.

Air mass C4, sampled at low altitude (~400 m), shows exposure to fossil fuel fluxes in Austria and Czech Republic (Fig. 6c). The mean observed slope is 3.2, close to the emission inventory ratio value for Czech Republic (4.4), while less close to the one from Austria (10.4). Thus, fossil fuel CO_2 from Czech Republic must dominantly influence these air masses. However, the large scatter around the linear regression line (R^2=0.47) indicates interplay of distinct combustion sources with different ratios.

Air mass C5 was sampled at quite low altitude (~400 m) over rural west Hungary. It is influenced by fluxes in West Hungary (local sources), as well in Austria, Switzerland and Southern Germany (remote sources). Despite the rather complex spiraling back-trajectories shown by Fig. 6d for C5, this air mass keeps a tight positive correlation between CO and CO_2, and the measured slope (8.93) is actually close to the regional inventory ratio (Hungary, Austria and Switzerland: ρ=10.1, 10.4 and 8.3, respectively).

In summary, this analysis shows that despite mixing of fossil CO_2 fluxes with biospheric CO_2 fluxes (which can be >0 in the North and <0 in the South in October; Fig. 1), and despite spatially and temporally variable CO:CO_2 fossil fuel combustion ratios in the different countries (which reflect different reliance on fossil fuel for energy

ACPD
10, 5665–5716, 2010

production), it is still possible at the scale of few days/hundreds of km to use the observed CO:CO_2 slope in atmospheric measurements to verify the contribution of fossil vs. other sources of CO_2. Here the integrative properties of synoptic atmospheric transport somehow help to average the contrasted CO:CO_2 ratios of local emissions.

5 Comparison of aircraft with surface stations measurements

Here we compare the aircraft measured CO_2 distribution with ground based station records. The goal is to produce a consistent 3-D picture of the CO_2 field, and to analyze the sources of concentration differences between altitude and ground level. We have the opportunity to use available CO_2 data from several ground based observatories at the time of the campaigns (CBW, PUY, CMN and PRS for CAATER-1; WES, HUN, SCH, PUY, CMN and PRS for CAATER-2 ; described in Table 3). Hourly data from the stations are selected from 12:00 to 18:00 UTC to filter out night-time and morning data, that are not representative of regional scale conditions (regional respiration fluxes).

Figure 9 provides a projection of Fig. 4 on the vertical longitude/altitude plan. It has been interpolated to produce vertical cross sections in Fig. 10. For interpolation, the 1 Hz data are first averaged into bins of 100 m altitude. Then a Delaunay triangulation in the altitude, longitude plane is applied (function TRIANGULATE of IDL package). After triangulation, the values are interpolated onto a regular grid (function TRIGRID of IDL package) at resolutions of 200 km in horizontal and 100 m in the vertical. In Fig. 10, the marine background value (let us recall these values: 374.5 ppm for CAATER-1; 367.9 ppm for CAATER-2) is removed from all the data. Figures 11 and 12 show a comparison between ground stations values and the mean profile recorded during each campaign.

The CO_2 vertical cross-sections (Fig. 10) show a strong variability into the atmospheric boundary layer (ABL) and more homogeneous values in the free troposphere (FT). This is true for both campaigns but even more for CAATER-1 than CAATER-2 (Figs. 11 and 12). Figure 10 shows that CO_2 into the CAATER-1 domain is globally

ACPD
10, 5665–5716, 2010

below the MBL value (374.5 ppm), whereas it is above the MBL background curve during CAATER-2 (367.9 ppm). One can also observe that CO_2 measured at the CARBOEUROPE stations CMN agrees better with the aircraft observation than the other stations, even if it is located outside the campaign domain. CO_2 at CMN (2165 m) compares within 0.7 ppm (0.3 ppm) to the CAATER-1 (CAATER-2) interpolated data at the stations location. During CAATER-1 (May 2001) the high diurnal cycle amplitude of CO_2 at CMN (http://gaw.kishou.go.jp/wdcgg/products/cd-rom/cd_14/A/metadata/co2/data/200612120073.html) reveals that this station lies within the ABL. However it is located at relatively high altitude and remote from local anthropogenic sources. During CAATER-2 it was located in the free troposphere and receving similar airmasses from the West, as the ones recorded during the closest profile around 12° E by the aircraft, on which mostly relies the interpolation at CMN. Interestingly, at PRS (4000 m) which was located in the free troposphere during both campaigns, interpolated airborne data and station observations are different from about 3 ppm and 0.5 ppm for CAATER-1 and CAATER-2, respectively. Indeed, the CAATER-1 interpolation lies on one profil done above northern Germany with air masses coming from the North (Fig. 5) while PRS is located much Southern and has encountering airmasses as well from South, East and West as it can be seen on Fig. 5. This reveals a gradient of a few ppm in the free troposphere over Western Europe.

CO_2 at surface stations CBW and WES is influenced by large nearby urban emissions, Amsterdam urban area and Northern Germany cities, and decoupled with the aircraft observation. CO_2 at CBW and WES (resp. WES and HUN) is more than 4 ppm higher (resp. 11 ppm) than the ABL value sampled by the aircraft during CAATER-1 (resp. during CAATER-2).

Comparison of aircraft data with mountain stations PUY and SCH is a little bit more complicated. Both stations are located on the top of mid-elevation mountains (1205 m a.s.l. and 1465 m a.s.l., respectively, for SCH and PUY) above urbanized valleys. During the morning and early afternoon, in spring and summer, SCH receives air advected by up-slope winds, delivering pollutants from valleys that have accumulated

during the night; and in the late afternoon, air is cleared out of this local influence under windy days (Schmidt et al., 2001). Therefore, CO_2 concentrations at SCH averaged between 12:00 UTC and 18:00 UTC will be less contaminated, but not exempt of urban pollution from the Rurh region cities. It matches very well the aircraft data during the CAATER-2 campaign (no data was available during CAATER-1). At PUY, local mesoscale circulations can either deliver pollution from Clermont-Ferrand city, or air from rural areas, depending upon the wind direction. Both at SCH and PUY, mixing of surface air with tropospheric air masses is thus always present, explaining why CO_2 at these stations are in-between the ABL and the FT (Fig. 10).

6 Analysis of the vertical variability

The CO_2 gradient between the boundary layer and the free troposphere is a key parameter to optimize fluxes with inverse methods. For each profile, the PBL height has been determined as the altitude at which the vertical gradient of the potential temperature begins to decrease, and where CO_2 and H_2O present step changes (Gerbig et al., 2003).

To illustrate the CO_2 vertical variability, the altitude of each single profile has then been normalized versus the PBL height; the normalized profiles are shown on Fig. 11 for CAATER 1 and CAATER 2. To improve readability, data have been averaged over 50 m layers.

As already noticed in the previous section, CO_2 shows a strong variability in the PBL comparing to the FT. The mean and standard deviation (std) computed on all data within the PBL are, respectively, 369.92 ppm and 3.99 ppm during CAATER 1; 371.55 ppm and 5.70 ppm during CAATER 2. In the FT, these values are 373.62 ppm and 0.49 ppm for CAATER 1; 371.2 ppm and 1.1 ppm for CAATER 2. In other terms, the atmospheric CO_2 variability over Europe is at least 5 to 8 higher in the PBL than in the FT.

ACPD
10, 5665–5716, 2010

The PBL variability is higher during the spring 2001 than during the fall 2002. Interestingly, the mean CO_2 jump is 3.7 ppm during CAATER 1 and −0.3 ppm during CAATER 2, with a similar FT averaged CO_2 concentration. Also, the mid PBL shows a minimum during CAATER 1 comparing to CAATER 2. These 2 points are the result of a higher photosynthetic activity during spring than during fall.

To go deeper into the variability analysis, on Figs. 12 and 13, all individual profiles have been plotted and colored in function of the location they have been recorded in and according to the origin of the air masses they come from as deduced from backplumes obtained with the LMDZ model, described in the companion paper (Xueref-Remy et al., 2010).

For CAATER 1, the CO_2 variability is very high in the first half of the PBL (355 to 378 ppm), with highest CO_2 values in the Brittany region due to local pollution from the Brest city area, and lowest values in the North of Germany with air depleted by the photosynthetic activity. In Southern and Eastern Germany, the vegetation seems less active but the signal does not contain urban pollution. In the mid troposphere, profiles recorded in Brittany come from air masses that travel between the ocean, the Channel sea and rural regions from North-West of France. CO_2 concentration range between 362 and 368 ppm, in function of the relative importance of continental air masses depleted by the photosynthetic activity comparing to oceanic air masses. In the FT, the atmosphere does not interact as much with ground sources and sinks, and the signal is thus constant.

For CAATER 2, the CO_2 variability in the first half of the PBL is lower than for CAATER 1 (364 to 381 ppm). The impact of the pollution from the Rühr region is visible on profiles recorded near the German-French border. Profile recorded in East Germany, close to Berlin, also show some local pollution. In the mid PBL, no depletion linked to the biospheric activity can be observed, as a difference from Spring 2001. The signal is quite homogeneous between the mid PBL and the FT. However, there is a striking zonal gradient in the CO2 mean mid-PBL concentration of about 11 ppm, revealing: 1) a weaker biospheric activity i.e. a Fall in advance in the West part of Europe

comparing to the East, 2) a higher mixing of continental and oceanic air in the West of Europe; and/or 3) higher CO_2 emissions in the West part of Europe such as in France comparing to the East part. Inventories from UNFCCC (2002) give 403.15 Mt CO_2/yr emitted by France against 863.88 Mt CO_2/yr emitted by Germany: this goes against hypothesis 3). However, inventories give 70.99 Mt CO_2/yr for Austria, 57.7 Mt CO_2/yr for Hungria, 16.29 Mt CO_2/yr for Slovenia, and 20.91 Mt CO_2/yr for Croatia. No data are available for the Federal Republic of Yugoslavia and Bosnia-Herzegovinia, but it is very likely that the total of the emissions from these countries (covered by the red region on Fig. 13) is less than the one from France: hypothesis 3) stands in this case. To infer the relative part of each hypothesis, we conclude that more regular aircraft measurements are needed in different sites of Europe. Such a program has been recently undertaken within the CARBOEUROPE-IP project (www.carboeurope.org) and upcoming publications on this will help to highlight our understanding of CO2 gradients in Europe.

7 Conclusion

This paper focuses on atmospheric CO_2 variability observed during the CAATER campaigns that occured above western Europe on 23–26 May 2001 (CAATER 1) and 2–3 October 2002 (CAATER 2) between the ground and 4000 m a.s.l. The instrumentation provided measurements of in-situ CO_2 (precision of 0.2 ppm), CO_2 flasks samples (precision of 0.1 ppm), Radon-222 (precision of 30%) during CAATER 1, and in-situ CO (precision of 5 ppb) during CAATER 2. Despite a stronger biogenic uptake in Spring, the lower troposphere mean level and the mean variability in May (370.1±4 ppm) is roughly similar in October (371.7±5 ppm). However, this mean value is lower than the marine background concentration for CAATER 1 (374.5 ppm) and higher for CAATER 2 (the marine background being more depleted, equaling 367.9 ppm). A backtrajectory analysis shows that during CAATER 1, dominant winds were coming from the northwest, while they were more balanced between the 4 sectors during CAATER 2.

During CAATER 1, the action of the biospheric sink over rural areas produced atmospheric CO_2 minima as low as 355 ppm, while the emissions from polluted regions such as Benelux and the Ruhr valley increased atmospheric CO_2 concentration to about 380 ppm around 1000 m a.s.l. above these regions.

During CAATER 2, CO_2 has been recorded simultaneously to CO (precision 5 ppb), which helped us to trace for fossil fuel emissions. After a classification of airmasses in function of their origin,we have calculated the ΔCO to ΔCO_2 ratio (Δ stands for the difference to the marine boundary layer concentration) and selected only well-identified polluted airmasses diagnosed from bak-trajectories. The polluted air masses show high R^2 values ranging from 0.33 to 0.88 and a large range of slope (2.42 to 10.37). Comparing these slopes to the ones from EMEP inventories for Western Europe countries, we have observed that it is possible to verify the contribution of fossil vs. other sources of CO_2 even at the scale of a few days or hundred of km.

Aircraft data have been compared to surface stations observations (CBW, PUY, CMN and PRS for CAATER 1; WES, HUN, SCH, PUY, CMN and PRS for CAATER 2). Only afternoon values have been selected to get data representative of the regional scale. Urban stations such as CBW and WES are strongly influenced by local emissions and decoupled with the airborne observations. Depending the time of the day and the meteorological situation, stations on top of small mountains such as SCH and PUY are located in the boundary layer (PBL) or in the free troposphere (FT); they match the airborne observations if in the FT and not contaminated by air uplifted from the valley. Stations in the FT and close to aircraft measurements such as CMN match quite well airborne measurements, as the atmosphere is well mixed at that altitude. However, PRS which is in the FT but a few 100 km further from the aircraft path differs of 3 ppm from the airborne measurements, which puts in light the existence of a CO_2 gradient of a few ppm above Europe in the FT.

As the gradient between the PBL and the FT is a key parameter for inverse modeling we have also analyzed CO_2 vertical variability. The mean jump between the PBL and the FT is of the order of 3.7 ppm during CAATER 1 and −0.3 ppm during CAATER 2,

ACPD
10, 5665–5716, 2010

and the variability is at least 5 to 8 times higher in the PBL than in the FT. Very striking is a strong zonal gradient during the CAATER 2 campaign in the CO_2 mean mid-PBL concentration (about 11 ppm), with higher concentrations in the west. This gradient could originate from a transport effect (a better mixing in the West of Europe), a Fall in advance in the West compared to the East, or higher emissions in the western countries than in the eastern countries of Western Europe. To better understand this gradient and discriminate correctly beween these hypothesis, more regular airborne vertical profiles are needed. Such a program has been undertaken in the framework of the CARBOEUROPE-IP project in 5 sites (Griffith, Scotland; Orleans, France; Hegyhatsal, Hungria ; Bialystok, Poland; and La Muela, Spain), with one flight every 5 days. The data are currently being analyzed and future publications on the way. In the companion paper (Xueref-Remy et al., 2010) we conduct a comparison of vertical profiles between models and observations. We also attempt to calculate CO_2 fluxes during the CAATER 1 campaign using the so-called "Radon method" based on simultaneous CO_2 and Radon-222 observations (Schmidt et al., 2003) and modeling tools.

Appendix A

NDVI maps for Western Europe during the CAATER campaigns

See Fig. A1.

Appendix B

Validation of the CO_2 in-situ analyser

As explained in Sect. 2, flasks measurements were compared to CONDOR measurements. We show here such a comparison for 26 May 2001 over Thüringen at

14:30 UTC, during which the Falcon flight was co-ordinated with those of a small aircraft equipped with a flask sampler from the MPI-BGC Jena group. LSCE flasks (circles), Jena flasks (triangles) and CONDOR (plain line) data agree within 0.2 ppm.

Acknowledgements. This work has been funded by the Institut National des Sciences de l'Univers, France, and by the European Commission in the framework of the AEROCARB project. We thank Ingeborg Levin and Martina Schmidt for helpful discussions on the Radon calculations. We thank David Picard for his participation to the campaign. NECP meteorological maps are due to Christopher Godfrey, the University of Oklahoma School of Meteorology, and the National Centers for Environmental Prediction/National Center for Atmospheric Research 40-Year Reanalysis Project. We thank Cyril Moulin and Fabienne Maignan from LSCE for providing NDVI maps. We are grateful to Nicolas Viovy for providing ORCHIDEE fluxes.

The publication of this article is financed by CNRS-INSU.

References

Andres, R. J., Marland, G., Fung, I., and Matthews, E.: A 1° × 1° distribution of carbon dioxide emissions from fossil fuel consumption and cement manufacture 1950–1990, Global Biogeochem. Cycles, 10, 419–429, 1996.

Baker, D. F., Doney, S. C., and Schimel, D. S.: Variational data assimilation for atmospheric CO_2, Tellus B, 58(5), 359–365, 2006.

Carouge, C., Bousquet, P., Peylin, P., Rayner, P. J., and Ciais, P.: What can we learn from European continuous atmospheric CO_2 measurements to quantify regional fluxes – Part 1: Potential of the network, Atmos. Chem. Phys. Discuss., 8, 18591–18620, 2008a, http://www.atmos-chem-phys-discuss.net/8/18591/2008/.

Carouge, C., Peylin, P., Rayner, P. J., Bousquet, P., Chevallier, F., and Ciais, P.: What can we learn from European continuous atmospheric CO_2 measurements to quantify regional fluxes – Part 2: Sensitivity of flux accuracy to inverse setup, Atmos. Chem. Phys. Discuss., 8, 18621–18649, 2008b, http://www.atmos-chem-phys-discuss.net/8/18621/2008/.

Crawford, J., Olson, J., Davis, D., Chen, G., Barrick, J., Shetter, R., Lefer, B., Jordan, C., Anderson, B., Clarke, A., Sachse, G., Blake, D., Singh, H., Sandolm, S., Tan, D., Kondo, Y., Avery, M., Flocke, F., Eisele, F., Mauldin, L., Zondlo, M., Brune, W., Harder, H., Martinez, M., Talbot, R., Bandy, A., and Thornton, D.: Clouds and trace gas distributions during TRACE-P, J. Geophys. Res, 108(D21), 8818, doi:10.1029/2002JD003177, 2003.

Drexler, R. R. and Hess, G. D.: An overview of the Hysplit 4 modelling system for trajectories, dispersion, and deposition, Austral. Met. Mag., 47, 295–308, 1998.

EMEP: Greenhouse gas emission trends and projections in Europe 2008, ISBN: 978-92-9167-981-2, vol. 5, 2008.

Filippi, D.: Etude et développement d'un instrument aéroporté destiné à la collecte des aérosols et à la mesure du Radon-222 par son dépôt actif, phD, Université Paris-6, 2000.

Filippi, D., Le Roulley, J. C., Ramonet, M., and Ciais, P.: Comprehensive greenhouse gases and radon profilings over Europe, 6th international Conference on CO_2, Sendai, Japan, October 2002.

Geels, C., Gloor, M., Ciais, P., Bousquet, P., Peylin, P., Vermeulen, A. T., Dargaville, R., Aalto, T., Brandt, J., Christensen, J. H., Frohn, L. M., Haszpra, L., Karstens, U., Rödenbeck, C., Ramonet, M., Carboni, G., and Santaguida, R.: Comparing atmospheric transport models for future regional inversions over Europe – Part 1: mapping the atmospheric CO_2 signals, Atmos. Chem. Phys., 7, 3461–3479, 2007, http://www.atmos-chem-phys.net/7/3461/2007/.

Gerbig, C., Schmitgen, S., Kley, D., Volz-Thomas, A., Dewey, K., and Haaks, D.: An improved fast-response vacuum-UV resonance fluorescence CO instrument, J. Geophys. Res., 104(D1), 1699–1704, 1999.

Gerbig, C., Lin, J. C., Wofsy, S. C., Daube, B. C., Andrews, A. E., Stephens, B. B., Bakwin, P. S., and Grainger, C. A.: Towards constraining regional-scale fluxes of CO_2 with atmospheric observations over a continent: 1. Observed Spatial Variability, J. Geophys. Res., 108, 4756, doi:10.1029/2002JD003018, 2003.

GLOBALVIEW-CO2: Cooperative Atmospheric Data Integration Project – Carbon Dioxide. CD-

ROM, NOAA GMD, Boulder, Colorado, also available on Internet via anonymous FTP to ftp.cmdl.noaa.gov, Path: ccg/co2/GLOBALVIEW, 2006.
GLOBALVIEW-CO: Cooperative Atmospheric Data Integration Project – Carbon Monoxide. CD-ROM, NOAA GMD, Boulder, Colorado, also available on Internet via anonymous FTP to ftp.cmdl.noaa.gov, Path: ccg/co/GLOBALVIEW, 2006.
Gloor, M., Fan, S. M., Pacala, S., and Sarmiento, J.: Optimal sampling of the atmosphere for purpose of inverse modelling - a model study, Global Biogeochem. Cycles, 14(1), 407–428, 2000.
Gurney, K. R., Law, R. M., Denning, A. S., Rayner, P. J., Baker, D., Bousquet, P., Bruhwiler, L., Chen, Y. H., Ciais, P., Fan, S., Fung, I. Y., Gloor, M., Heimann, M., Higuchi, K., John, J., Kowalczyk, E., Maki, T., Maksyutov, S., Peylin, P., Prather, M., Pak, B. C., Sarmiento, J., Taguchi, S., Takahashi, T., and Yuen, C. W.: TransCom 3 CO_2 inversion intercomparison: 1. Annual mean control results and sensitivity to transport and prior flux information, Tellus, 55B(2), 555–579, 2003.
Gurtney, K. R., Law, R., Denning, A. S., et al.: Transcom 3 inversion intercomparison: Model mean results for the estimation of seasonal carbon sources and sinks, Global Biogeochem. Cycles, 18, GB1010, doi:10.1029/2003GB002111, 2004.
Intergovernmental Panel on Climate Change: IPCC Climate Change 2007: The Scientific Basis, Cambridge Univ. Press, New York, 2007.
Karstens, U., Gloor, M., Heimann, M., and Rödenbeck, C.: Insights from simulations with high-resolution transport and process models on sampling of the atmosphere for constraining mid-latitude land carbon sinks. J. Geophys. Res., 111, D12301, doi:10.1029/2005JD006278, 2006.
Krinner, G., Viovy, N., De Noblet-Ducoudré, N., Ogée, J., Polcher, J., Friedlingstein, P., Ciais, P., Sitch, S., and Prentice, I. C.: A dynamic global vegetation model for studies of the coupled atmosphere-biosphere system, Global Biogeochem. Cycles, 19, GB1015, doi:10.1029/2003GB002199, 2005.
Kritz, M. A. and Rosner, S. W.: Validation of an off-line three-dimentional chemical transport model using observed radon profiles, J. Geophys. Res., 103(D7), 8425–8432, 1998.
Law, R. M., Peters, W., Rodenbeck, C., and TRANSCOM contributors: TransCom model simulations of hourly atmospheric CO_2 : experimental overview and diurnal cycle results for 2002, Global Biogeochem. Cycles, 22, GB3009, doi:10.1029/2007GB003050, 2008.
Levin, I. and Karstens, U.: Inferring high-resolution fossil fuel CO_2 records at continental sites

from combined 14CO_2 and CO observations, Tellus, 59B, 245–250, doi:10.1111/j.1600-0889.2006.00244.x, 2007.

Nedelec, P., Cammas, J.-P., Thouret, V., Athier, G., Cousin, J.-M., Legrand, C., Abonnel, C., Lecoeur, F., Cayez, G., and Marizy, C.: An improved infrared carbon monoxide analyser for routine measurements aboard commercial Airbus aircraft: technical validation and first scientific results of the MOZAIC III programme, Atmos. Chem. Phys., 3, 1551–1564, 2003, http://www.atmos-chem-phys.net/3/1551/2003/.

Palmer, P. I., Suntharalingham, P., Jones, D. B. A., Jacob, D. J., Streets, D. G., Fu, Q., Vay, S., and Sachse, G. W.: Using CO_2:CO correlations to improve inverse analyses of carbon fluxes, J. Geophys. Res., 111, D12318, doi:10.1029/2005JD006697, 2006.

Paris, J.-D., Ciais, P., Nedelec, P., Ramonet, M., Belan, Yu, M., Arshinov, M., Golytsin, G. S., Granberg, I., Stohl, A., Cayez, G., Athier, G., Boumard, F., and Cousin, J. M.: The YAK-AEROSIB transcontinental aircraft campaigns: new insights on the transport of CO_2, CO and O_3 across Siberia, Tellus B, 60(4), 551–568, 2008.

Patra, P. K., Law, R. M., Peters, W., et al.: TransCom model simulations of hourly atmospheric CO_2 : analysis of synoptic-scale variations for the period 2002–2003, Global Biogeochem. Cycles, 22, GB4013, doi:10.1029/2007GB003081, 2008.

Pépin, L., Schmidt, M., Ramonet, M., Worthy, D., and Ciais, P.: A new gas chromatographic experiment to analyze greenhouse gases in flask samples and in ambient air in the region of Saclay, Notes Instrumentales IPSL no. 13, 2001.

Ramonet M., Ciais, P., Nepomniachii, I., Sidorov, K., Neubert, R. E. M., Langendörfer, U., Picard, D., Kazan, V., Biraud, S., Gusti, M., Kolle, O., Schulze, E. D., and Lloyd, J.: Three years of aircraft-based trace gas measurements over the Fyodorovskoye southern taiga forest, 300 km north-west of Moscow, Tellus, 54B, 713–734, 2002.

Rivier, L., Ciais, P., Hauglustaine, D.A., Bakwin, P., Bousquet, P., Peylin, P., and Klonecki, A.: Evaluation of SF_6, C_2Cl_4 and CO to approximate fossil fuel CO_2 in the Northern Hemisphere using a chemistry transport model, J. Geophys. Res. 111, D16311, doi:10.1029/2005JD006725, 2006.

Schmidt, M., Glatzel-Mattheier, H., Sartorius, H., Worthy, D. E., and Levin, I.: Western European N_2O emissions : A top-down approach based on atmospheric observations, J. Geophys. Res., 106(D6), 5507–5516, 2001.

Schmidt, M., Graul, R., Sartorius, H., and Levin, I.: The Schauinsland CO_2 record : 30 years of continental observations and their implications for the variability of the European CO_2

budget, J. Geophys. Res., 108(D19), 4619–4626, 2003.
Stephens, B. B., Gurney, K. R., Tans, P. P., Sweeney, C., Peters, W., Bruhwiler, L., Ciais, P., Ramonet, M., Bousquet, P., Nakazawa, T., Aoki, S., Machida, T., Inoue, G., Vinnichenko, N., Lloyd, J., Jordan, A., Heimann, M., Shibistova, O., Langenfelds, R. L., Steele, L. P., Francey, R. J., and Denning, A. S.: Weak Northern and Strong Tropical Land Carbon Uptake from Vertical Profiles of Atmospheric CO_2, Science, 316(5832), 1732–1735, doi:10.1126/science.1137004, 2007.
Suntharalingam, P., Jacob, D. J., Palmer, P. I., Logan, J. A., Yantosca, R. M., Xiao, Y., Evans, M. J., Streets, D. G., Vay, S. L., and Sachse, G. W.: Improved quantification of Chinese carbon fluxes using CO2/CO correlations in Asian outflow, J. Geophys. Res., 109, D18S18, doi:10.1029/2003JD004362, 2004.
Takahashi, T., Wanninkhof, R. H., Feely, R. A., Weiss, R. F., Chipman, D. W., Bates, N., Olafsson, J., Sabine, C., and Sutherland, S. C.: Net sea-air CO_2 flux over the global oceans: An improved estimate based on the air-sea pCO_2 difference, in 2nd CO_2 in ocean symposium, Tsukuba, Japan, 18–23 January 1999.
Takahashi, T., Sutherland, S. C., Sweeney, C., Poisson, A., Metzl, N., et al.: Global Sea-Air CO_2 Flux Based on Climatological Surface Ocean pCO_2, and Seasonal Biological and Temperature Effect, Deep Sea Res. II, 49(9–10), 1601–1622, 2002.
Xueref-Remy, I., Bousquet, P., Carouge, C., Rivier, L., Viovy, N., and Ciais, P.: Variability and budget of CO_2 in Europe: analysis of the CAATER airborne campaigns – Part 2: Comparison of CO_2 vertical variability and fluxes from observations and a modeling framework, Atmos. Chem. Phys. Discuss., 10, 4271–4304, 2010, http://www.atmos-chem-phys-discuss.net/10/4271/2010/.

Table 1. Airport acronyms and geographical information.

Code	Name	Country	Latitude	Longitude	Altitude (m a.s.l.[a])
BZH	Brest	France	48°26′ N	04°25′ W	99
HUN	Hegyhatsal	Hungary	46°58′ N	16°39′ E	250
OBP	Oberpfaffenhofen	Germany	48°05′ N	11°17′ E	593
ORL	Orleans	France	47°53′ N	02°10′ E	120
PDB	Paderborn	Germany	51°36′ N	08°37′ E	213

[a] m a.s.l.=meters above sea level

ACPD
10, 5665–5716, 2010

Table 2. Flight information for the CAATER 1 and CAATER 2 campaigns.

Date	Time range (UTC)	Flight pattern	Flight number
23 May 2001	12:12–14:43	OBP–BZH	1
24 May 2001	15:03–17:50	Atlantic, south of BZH	2
25 May 2001	11:26–13:43	BZH–PDB	3
26 May 2001	08:56–15:46	PDB–OBP	4
2 Oct 2002	08:48–11:10	OBP–ORL	5
2 Oct 2002	11:10–13:16	ORL–PDB	6
3 Oct 2002	10:02–12:20	PDB[a]–HUN	7
3 Oct 2002	14:19–15:52	HUN–OBP	8

[a] No data available between PDB and THU.

ACPD
10, 5665–5716, 2010

Table 3. Ground station acronyms and geographical information.

Site	Name	Country	Latitude	Longitude	Altitude (m a.s.l.[a])	Type
CBW	Cabauw	Netherlands	51°58′ N	04°55′ E	213	Tower (20 m)
CMN	Monte Cimone	Italy	44°11′ N	10°42′ E	2165	Moutain
HUN	Hegyhatsal	Hungary	46°57′ N	16°39′ E	115	Tower (115 m)
MHD	Mace Head	Ireland	53°19′ N	09°53′ W	26	Surface
PRS	Plateau Rosa	Italy	45°56′ N	07°42′ E	3480	Moutain
PUY	Puy-de-Dome	France	45°45′ N	03°00′ E	1465	Mountain
SCH	Schauinsland	Germany	47°55′ N	07°55′ E	1205	Moutain
WES	Westerland	Germany	54°56′ N	08°19′ E	12	Surface

[a] m a.s.l. = meters above sea level

ACPD
10, 5665–5716, 2010

Table 4. Characteristics of the CO_2 and CO analyzers.

Parameter	CO_2 analyzer (CONDOR)	CO analyzer
Precision	≤ 0.20 ppm for 1 s	±5 ppbv for 30 s
Sampling frequency	1 Hz	0.03 Hz
Power supply	18–32 V DC/15 A max	24 V/10 A max
Cells pressure	1080 hPa	2532 hPa
Flow rates	50 sccm (Reference cell) 400 sccm (Sample cell)	4000 sccm
Temperature	35 °C	30
Calibrations	1 calibration (6 min) every 30 min	Before and after each campaign
Volume	95×55×40 cm^3	60×31×43 cm^3
Weight	80 kg	45 kg

Table 5. Evaluation of the correlation level between CO_2 and CO for the different events selected from Fig. 7. Each event has been attributed to a class according to its backtrajectories location and direction (from Fig. 6) as explained in the text.

Event	Determination factor R^2	Slope $\delta\Delta CO/\delta\Delta CO_2$	Day (in Oct 2002)
C1	0.82	6.38	2
C2	0.65	3.52	2
C3	0.26	1.78	3
C4	0.47	3.2	3
C5	0.69	8.93	3
M1	0.13	0.9	2
M2	0.35	0.76	2
M3	−0.42	−2.88	2
M4	−0.06	−0.36	2
B1	−0.67	−11.4	2
B2	0.54	12.1	2
B3	−0.41	−10.1	2
B4	0.15	3.56	3
B5	−0.56	−7.15	3
B6	−0.43	−2.56	3
B7	−0.73	−2.36	3

ACPD
10, 5665–5716, 2010

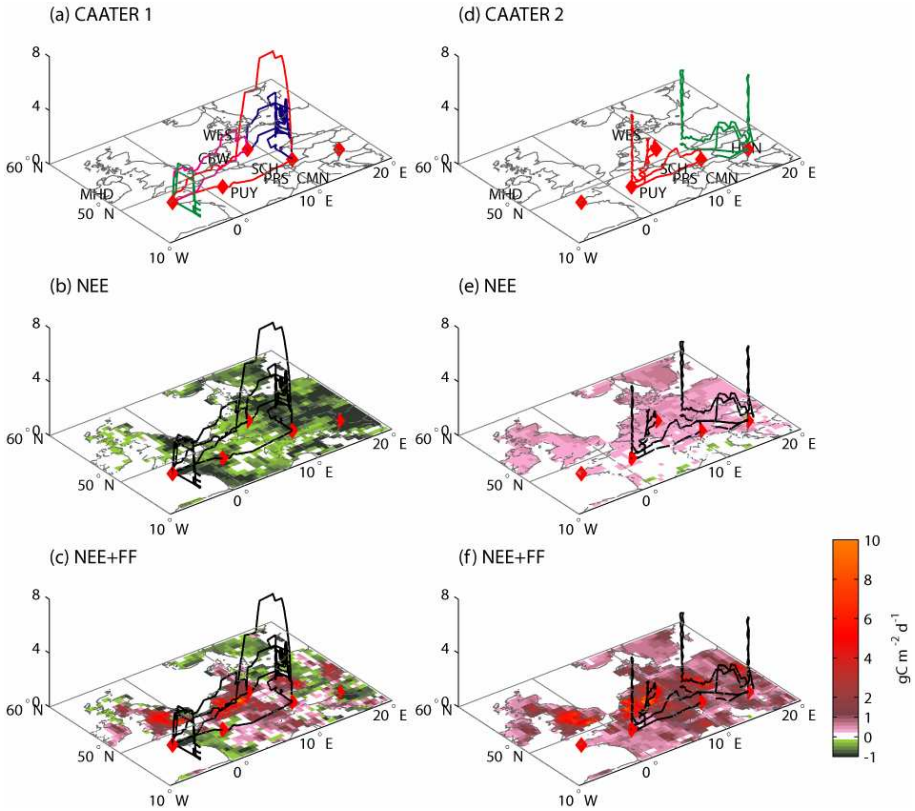

Fig. 1. Averaged flux maps (on the days of the campaigns) and flight patterns (red: 1st day, green: 2nd day, pink: 3rd day, blue: 4th day of the campaigns) in function of latitude, longitude and altitude (in km). Net Ecosystem Exchange (NEE) fluxes are from ORCHIDEE and fossil fuel (FF) fluxes from ANDRES (left: CAATER 1, right: CAATER 2). Oceanic fluxes are almost zero and thus do not appear in the figure.

ACPD
10, 5665–5716, 2010

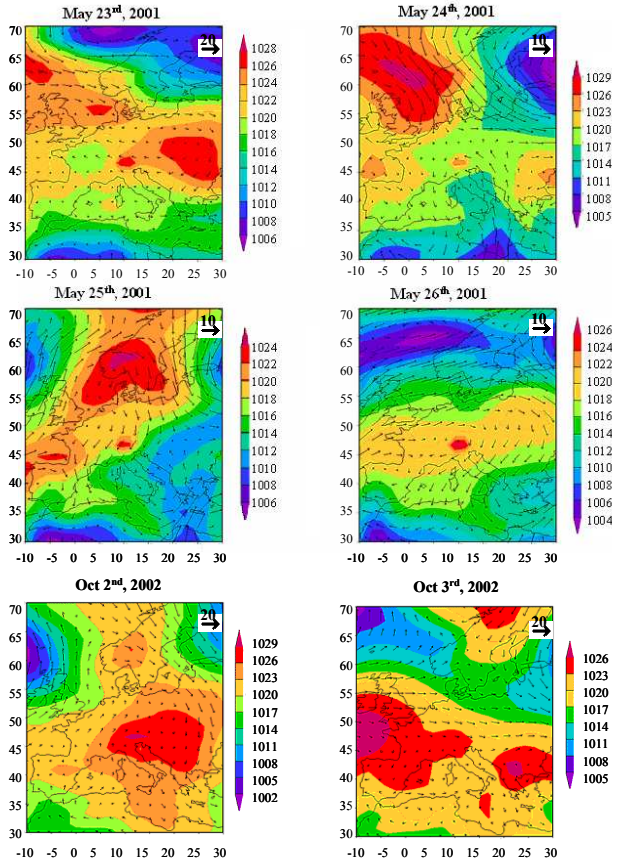

Fig. 2. Meteorological maps showing mean sea-level pressure (in hPa) and wind speed (in $m\,s^{-1}$) at 850 hPa for each day of the CAATER campaigns at 12:00 GMT (http://weather.ou.edu/~cgodfrey/reanalysis/). Latitudes (horizontal scale) are given in ° E and longitudes (vertical scale) in ° N.

ACPD
10, 5665–5716, 2010

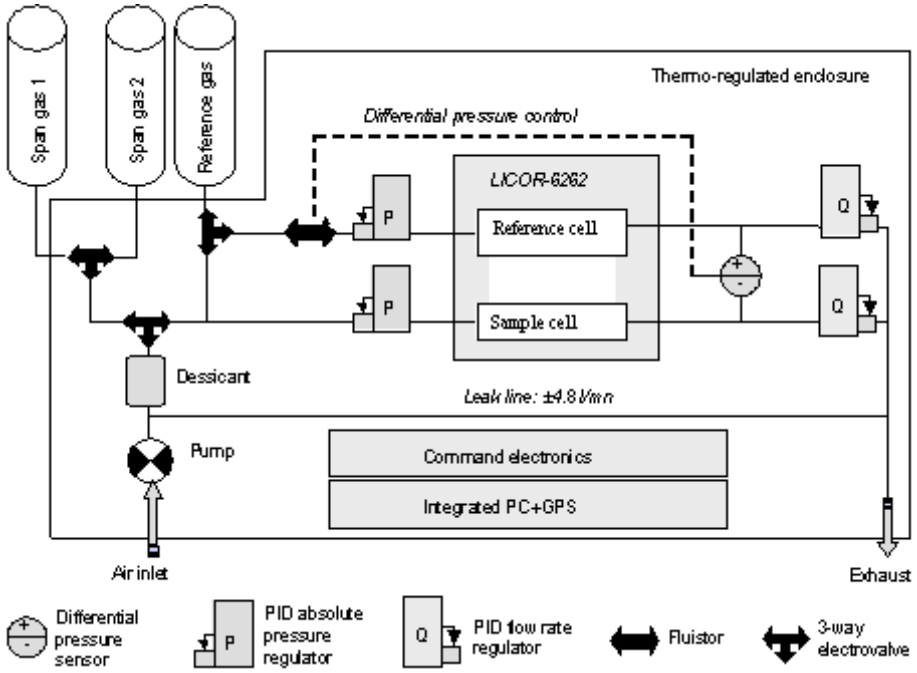

Fig. 3. Schematic of the CONDOR analyzer.

ACPD
10, 5665–5716, 2010

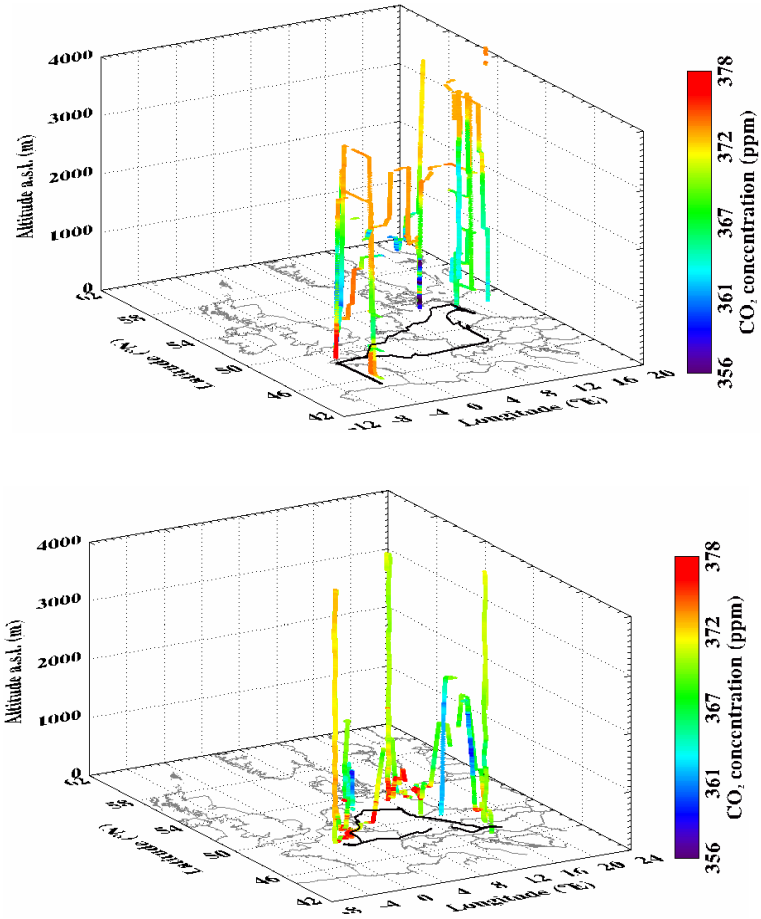

Fig. 4. CO_2 concentration 3-D distribution in function of longitude, latitude and altitude. The flight patterns are projected on the latitude/longitude plane (top: CAATER 1, bottom: CAATER 2).

ACPD
10, 5665–5716, 2010

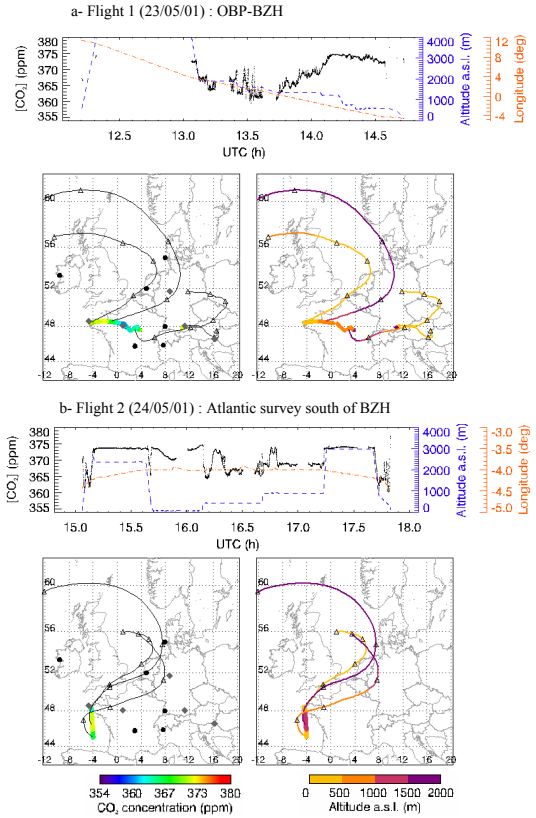

Fig. 5. Backtrajectories computed over 96 h for flight 1 and flight 2. The distance between 2 triangles is 24 h. Left panels show CO_2 concentrations along the flight path and backtrajectories. Right panels show the altitude of the flight, and backtrajectories colored in function of the air mass altitude. Black circles represent ground stations which names are given in Fig. 1. Altitude is given above sea level (a.s.l.). Note that some of the backtrajectories go outside of the latitude and longitude chosen borders, but these are so much diluted that they do not give any relevant information.

ACPD
10, 5665–5716, 2010

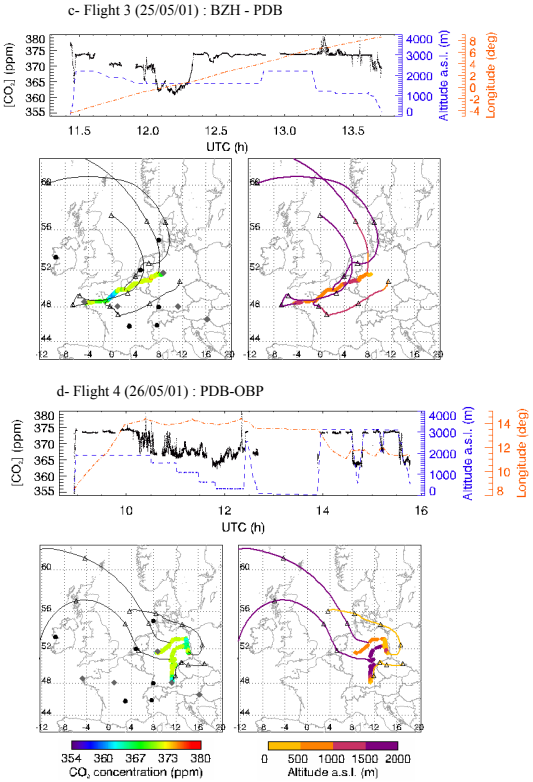

Fig. 5. Backtrajectories computed over 96 h for flight 3 and flight 4. The distance between 2 triangles is 24 h. Left panels show CO_2 concentrations along the flight path and backtrajectories. Right panels show the altitude of the flight, and backtrajectories colored in function of the air mass altitude. Black circles represent ground stations which names are given in Fig. 1. Altitude is given above sea level (a.s.l.). Note that some of the backtrajectories go outside of the latitude and longitude chosen borders, but these are so much diluted that they do not give any relevant information.

ACPD
10, 5665–5716, 2010

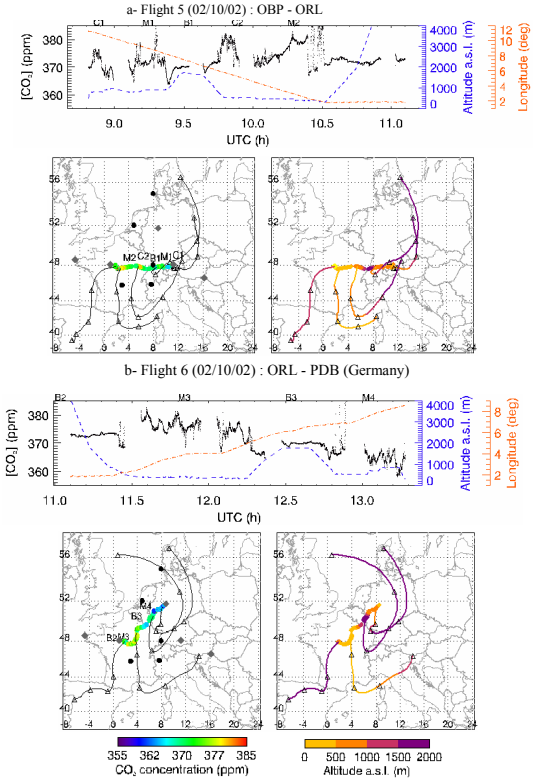

Fig. 6. Backtrajectories computed over 96 h on the 2 October 2002 flights (**a** before 11:10, **b** after 11:10). The distance between 2 triangles is 24 h. Left panels show CO_2 concentrations along the flight path and backtrajectories. Right panels show the altitude of the flight, and backtrajectories colored in function of the air mass altitude. Black circles represent ground stations which names are given in Fig. 1. Altitude is given above sea level (a.s.l.). Note that some of the backtrajectories go outside of the latitude and longitude chosen borders, but these are so much diluted that they do not give any relevant information.

ACPD
10, 5665–5716, 2010

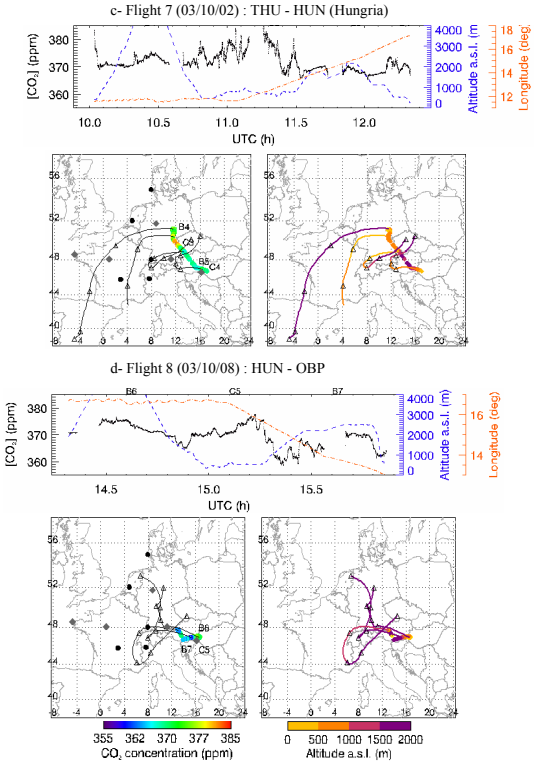

Fig. 6. Backtrajectories computed over 96 h on the 3 October 2002 flights (**c** before 12:30, **d** after 12:30). The distance between 2 triangles is 24 h. Left panels show CO_2 concentrations along the flight path and backtrajectories. Right panels show the altitude of the flight, and backtrajectories colored in function of the air mass altitude. Black circles represent ground stations which names are given in Fig. 1. Altitude is given above sea level (a.s.l.). Note that some of the backtrajectories go outside of the latitude and longitude chosen borders, but these are so much diluted that they do not give any relevant information.

ACPD
10, 5665–5716, 2010

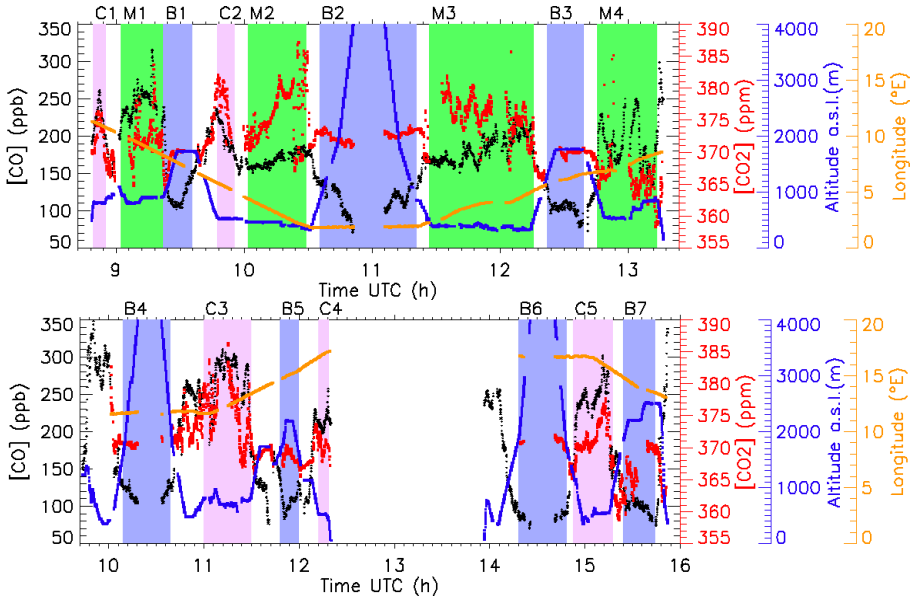

Fig. 7. CO, CO_2 and altitude time series during the CAATER 2 flights (top: 2 October; bottom: 3 October). Striking events have been selected with colorbars (pink is for C: high CO and CO_2 correlation level events, green is for M: mixed determination factor events, blue is for B: tropospheric background events).

ACPD
10, 5665–5716, 2010

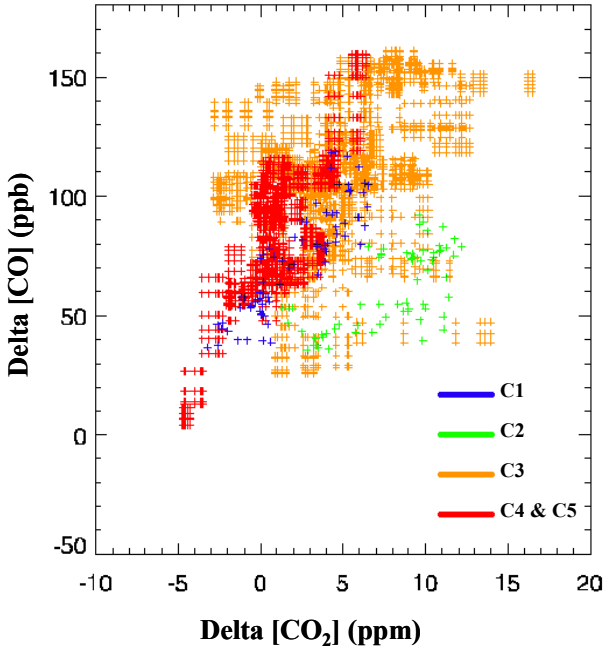

Fig. 8. ΔCO (i.e. CO minus CO MBL background) versus ΔCO_2 (i.e. CO_2 minus CO_2 MBL background) for the CAATER 2 flights (left: 2 October 2002, right: 3 October 2002). Colors represent correlated events C1 to C5 defined in the text.

ACPD
10, 5665–5716, 2010

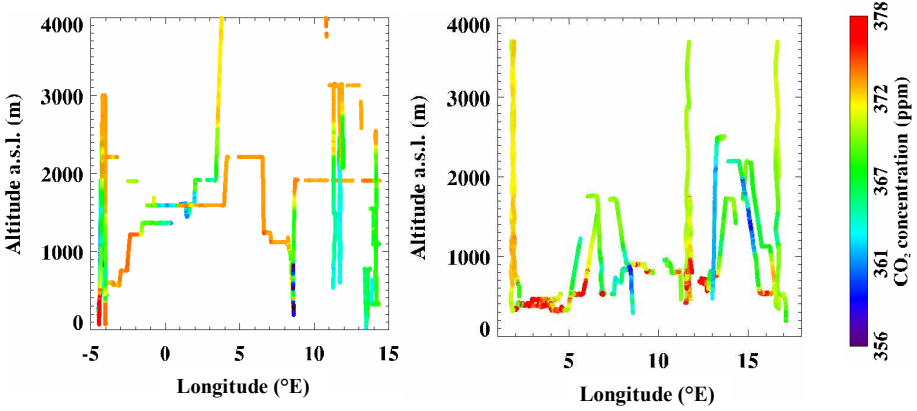

Fig. 9. CO_2 concentrations along the flight patterns represented in function of altitude and longitude during the CAATER 1 (left) and CAATER 2 (right) campaigns.

ACPD
10, 5665–5716, 2010

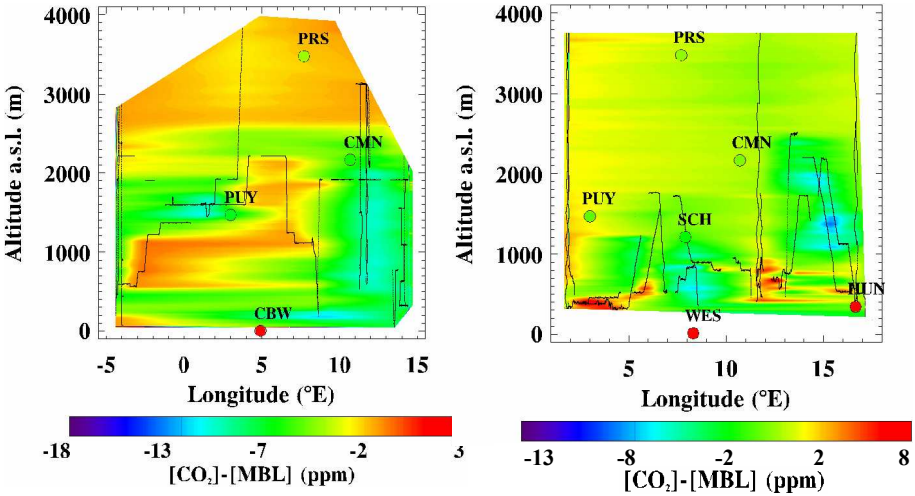

Fig. 10. Interpolation of the CO_2 concentrations for the whole campaign and for each leg in function of altitude and longitude during the CAATER 1 (left) and CAATER 2 (right) campaigns. The concentration scale is referred to the MBL background concentration of each campaign, as defined in the text. Flight paths are shown in black. Ground stations concentrations, averaged as described in Sect. 1, are shown at the respective station coordinates. Note that for plot convenience, HUN and WES stations during CAATER 2 are shown as being on the maximum of the chosen concentration scale, while indeed they show even higher concentrations (respectively: 12.72 ppm and 38.47 ppm above MBL background concentration).

ACPD
10, 5665–5716, 2010

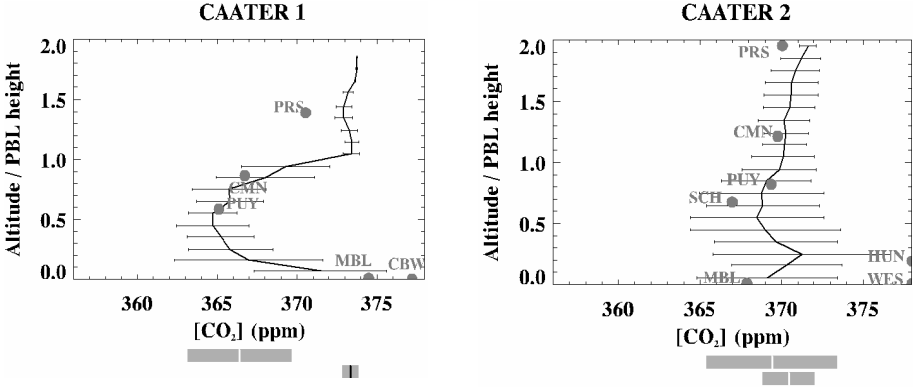

Fig. 11. Variability observed in the PBL and the FT during each campaigns (left: CAATER 1, right: CAATER 2) using profiles only. The altitude of each individual profiles has been normalized to the relevant PBL height. The plot shows the mean and standard deviation (1-s) of CO2 concentration over layer of 1/10th of the PBL height. The global mean and variability (±1-s standard deviation) in the PBL (upper grey bar) and FT (lower grey bar) are shown according to the CO_2 concentration scale of the plot.

ACPD
10, 5665–5716, 2010

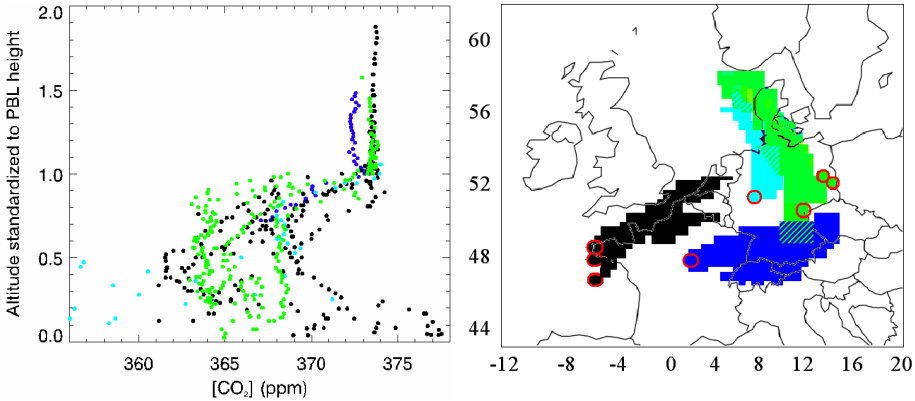

Fig. 12. CAATER 1 vertical variability analysis. Left panel: all CO_2 profiles binned over 50 m layers and standardized to their respective PBL height. Right panel: schematic of the regions covered by the backtrajectories of the profiles (profile locations are indicated by circles). Colors of right and left panels correspond one to each other.

ACPD
10, 5665–5716, 2010

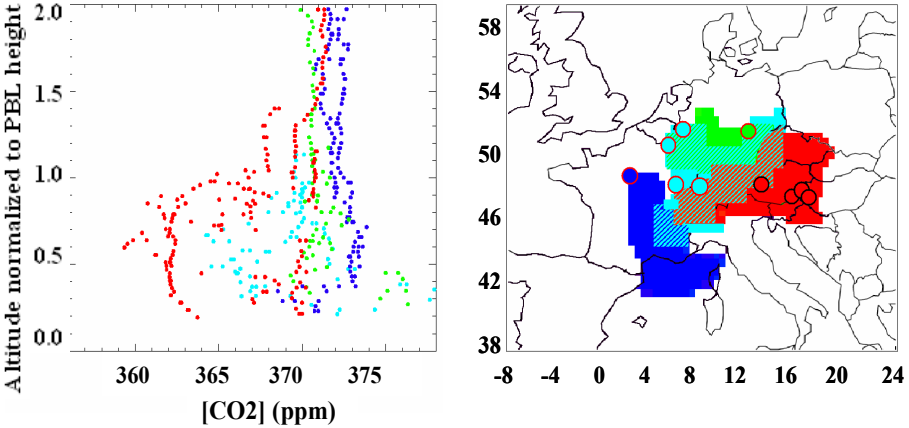

Fig. 13. CAATER 2 vertical variability analysis. Left panel: all CO_2 profiles binned over 50 m layers and standardized to their respective PBL height. Right panel: schematic of the regions covered by the backplumes associated to the profiles (profile locations are indicated by circles). Colors of right and left panels correspond.

ACPD
10, 5665–5716, 2010

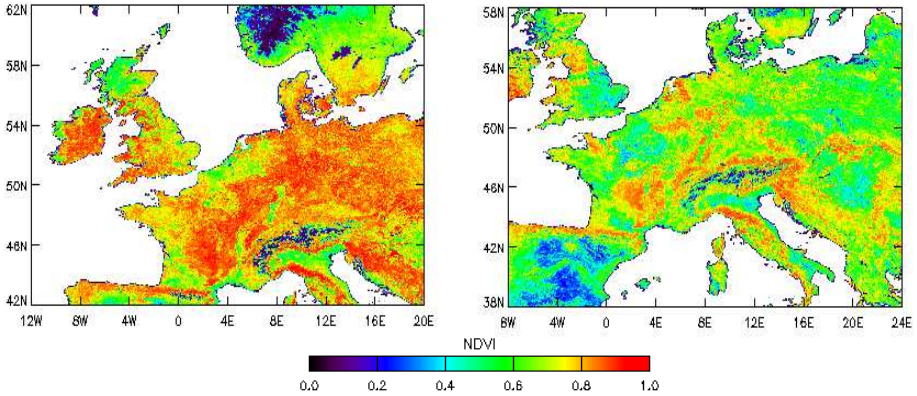

Fig. A1. NDVI maps on 21 May 2001 for CAATER 1 (left) and on 1 October 2002 for CAATER 2 (right).

ACPD
10, 5665–5716, 2010

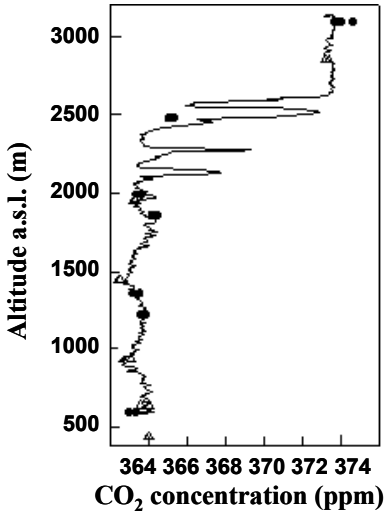

Fig. B1. Coordinated flights over Thringen on 26 May 2001 at 14:30 UTC (in-situ: plain line, LSCE flasks: plain circles; Jena flasks: opened triangles).

ACPD
10, 5665–5716, 2010